Intelligent 3-stage Lead Acid Battery Auto Charger

Abdul Quader Munshi[1+], Kazi Abu Sayeed[1], Monalisha Mishu[2]

[1]Department of EECS, North South University,

Bashundhara R/A, Dhaka, Bangladesh.

[2]Department of ETE, Daffodil International University,

Dhanmondi, Dhaka, Bangladesh.

Abstract. This document reports a programmable intelligent three-stage lead acid battery charger where the traditional linear power regulator is replaced by an advanced buck-converter, which works as a programmable and variable switching regulator, which varies the output automatically as per the programmed logic for charging batteries. As a switching regulator, it also increases the over-all efficiency than traditional chargers. Also this buck-converter is modified by replacing the freewheeling diode of it by an n-MOSFET to increase the efficiency further. And the p-MOSFET of the buck-converter reference design has been replaced by another n-MOSFET to reduce cost. To reduce the cost further, a micro-controller is used instead of a regular PWM driver. Overall, this device is low cost and manufacturable with most commonly available components in the market of Bangladesh.

Keywords: Battery charger, Buck-converter, n-MOSFET, Micro-controller, Low cost

1. Introduction

There are various ways of charging Lead Acid Batteries. But the best option for a Lead Acid battery is using the 3stage charging, that involves Bulk Current as first stage and then Topping Charge at a constant voltage and finally a Float Charge at a lower but constant voltage.[1] For a 12V, 6 cells lead acid battery, we can get the following data.[2]

Table I Per Plate Voltage of Different Stage of Charging

Min volt/cell	Bulk current mode (volt/cell)	Topping volt/cell	Float volt/cell
2.1	2.1-2.4	2.4-2.45	2.25-2.3
	Stage 1	Stage 2	Stage 3

Also while charging, we must take the battery terminal temperature, T_{bat} into account and compensate the charging voltage for stage 2 and 3 according to the temperature. Ref [5] gives us a hint on what should be our volt/cell for charging stage 2 and 3, which gives us two simple functions for charging stage 2 and 3. Those are:

$V_{top} = 15.15 - (0.03 \times T_{bat})$ ---(Eq. 1)

$V_{float} = 14.15 - (0.03 \times T_{bat})$ ---(Eq. 2)

[+] Corresponding author. *E-mail address*: [1]a.quader@banglardamal.org,
[1]kazisayeed@northsouth.edu, [2]monalisha@banglardamal.org.

Let us consider a 7Ah lead acid battery as a sample, with C rating of 0.1C as our charging current I_{chrg} = 700mA (i.e. charging current is $1/10^{th}$ of the total battery capacity in Ampere). Note that, the battery manufacturers generally supply C rating and 0.1C is a common practice. We will supply I_{chrg} amount of current to a fully discharged (i.e. V_{bat} = 10.5V or 1.75V/cell) or low charged (i.e. $10.5V < V_{bat} < 11.7V$) battery until the voltage of the battery reaches the stage 2 level. As soon as it does, we move from the constant current mode to constant voltage mode. If the battery voltage is already 11.7V (1.95V/cell), we can skip stage 1 and move to stage 2. Note that, charging at bulk current at this level of voltage may reduce the battery lifetime. Also note that during charging, V_{bat}, I_{chrg} and T_{bat} will be continuously monitored.
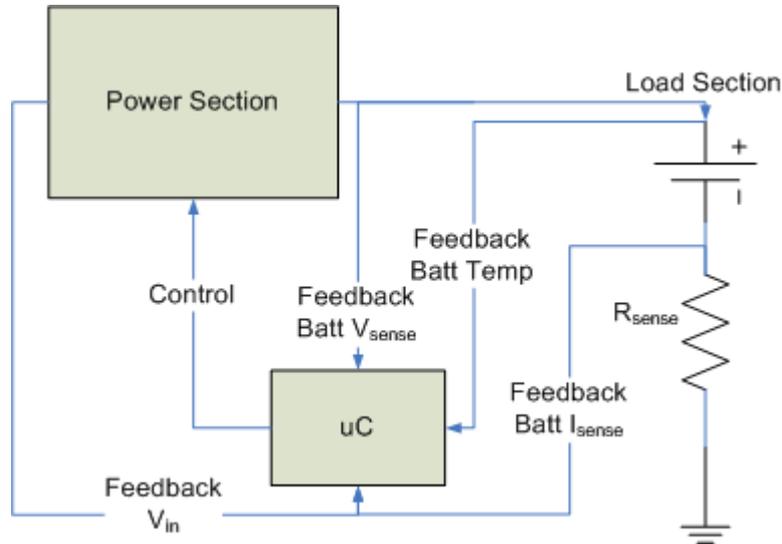

Fig. 1 Block diagram of the entire system.

Once the V_{bat} reaches to 14.4V (2.4V/cell), we will enter in to the step 2, *topping charge mode* which will supply a constant voltage, V_{top} = 14.4V (2.4V/cell). This time, we will still continue to monitor the V_{bat}, T_{bat} and I_{chrg} and we will change the V_{top} according to the equation (1). At this stage, we will compare the I_{chrg} to the threshold of I_{th} = 2% of battery capacity, (i.e. 2% of 7A = 140mA).

If $I_{chrg} <= I_{th}$ then we will move to step 3, *float charge mode* where a constant voltage V_{float} = 13.4V to 13.5V (2.25V/cell) will be applied to the battery and still the V_{bat}, T_{bat} and I_{chrg} will be monitored and V_{float} will be adjusted according to equation (2). As this is the last stage of our charging, we can assume that the battery is almost fully charged and we can either disconnect or keep it connected at this stage, as float mode will always compensate with self-discharge of the battery and will keep the battery in a healthy condition without over charge.[2]

2. Description of Device

The device can be divided in the following blocks: *power section, control section, sensing and feedback, load*. Fig. 1 shows the entire connectivity between the different blocks of the system.

2.1. Power Section

This is basically a buck-converter. The reference model for this particular battery charger was taken from [4] with some minor changes on it. Fig. 2 is the modified version of the reference design given at [4], where the p-MOSFET (P1 of Fig. 1 in [4]) has been replaced by an n-MOSFET (Q1). Also the freewheeling diode D has been replaced by another n-MOSFET (Q2) as per [4], which also appears at [10]. As [4] gives us the hint of the effect of using a general diode, an schottkey diode and a MOSFET. As MOSFET has low Rds, we will use an n-MOSFET instead of the diode utilizing the body diode of the FET, which will give us the most efficiency compare to diodes. For relevant mathematical calculations, please see Appendix – I

2.2. Control Section

This is consisting of a very popular and easy to find microcontroller (μC), AtMega8 from Atmel Corporation. This μC will be the heart of the whole charger, as this will decide and do all the necessary works to drive the buck-converter based on the readings from *sensing and feedback*.
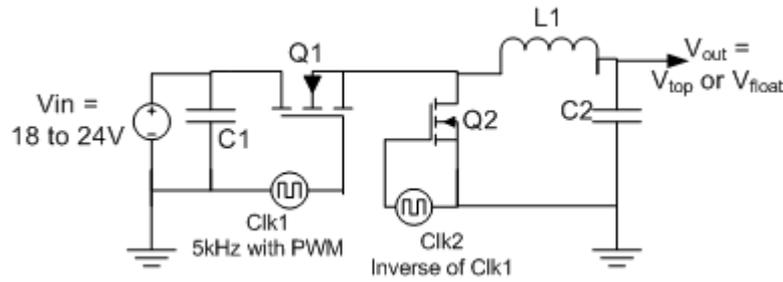

Fig. 2 Detail of power section.

2.3. Sensing and Feedback

It consists several sensors like current sensor for load's current consumption, voltage sensing for battery terminal voltage, output voltage from the power section, input voltage to the power section and temperature sensing. All of the sensing data will be transferred to μC for calculation and to determine the best condition for charging the battery.

2.4. Load

This is basically the battery/battery bank that we intend to charge. But while designing, we have to fix the *load* to a particular value or we have to choose a range of load while designing the charger, as based on the *load* several parameters related to control of the charging V-I and system capacity will change.

3. Device Operation

Ref [8] gives us the total idea of a buck-converter and as we are replacing the freewheeling diode with Q2, we have to turn ON Q2 also at the time when the Diode is supposed to conduct. As enhancement type FETs (like IRF540 or IRFZ44N which are low cost and easily available at the local market of Bangladesh) has built in parasitic body diode, it will automatically work for any situation of reverse bias when the FET is off. But in the case of forward bias, the FET must be turned ON. This means as we are using clocks with PWM for controlling current coming in to the L [Fig 2], we have to use a clock source that we will apply at the gate of Q1. But when Q1 is ON, the diode in the buck-converter, which is replaced by the n-MOSFET Q2 in our case must be reversed biased, means OFF. And when Q1 is OFF, the Q2 then has to be ON. Thus at Q2, we will apply a complement of the PWM clock, that we will apply at Q1.

The two signals at Q1 and Q2, which are complement of each other, must be well synchronized. This can be done using either a relatively fast inverter (any fast switching inverter is fine, regardless of BJT/logic gate) where the clock for Q1 will be simultaneously inverted and then will be fed in to Q2 as its clock. Also we can do this using software control, as ATMega8 has three PWM channels and we need two. For both the cases, the inversion speed or instruction execution time must be relatively very higher compare to the actual PWM clock. Failure to do so will accidentally turn ON the Q2 while Q1 is still ON and that will lead to a short circuit path directly to device ground even bypassing the L. To solve this, we have to select a clock of somewhere in kHz range where the inverter or software execution will be at MHz range. However, as using software, it is easier to do calibration by inserting only some correction codes, software driven inversion is more preferable than hardware inverter.

Fig 1. tells us that the device is feedback oriented. Several sensors are used at several locations to give various data to the μC. μC will measure the voltage after L as V_{out} when Q1 and Q2 are ON as V_{bat} when they are OFF. In addition, through the entire time of operation it will continuously measure V_{in}. Also when Q1 is on, it will measure V_{out} for V_{bat} or V_{top} or V_{float} based on the operating stage 1, 2 and 3. Also μC will measure the T_{bat} at the same location. The charging current, I_{chrg} will be measured from a shunt resistor R_{sense} after the load (battery). In this case we are using low-side current measuring.[9] The shunt resistor here has been proposed to be a 0.1ohm 5W ceramic resistor, which is again available in the local market.

As the device is a controllable buck-converter, the μC will constantly measure different parameters and will set appropriate PWM duty for stage 2 and 3 to supply a constant voltage according to equation (1) and (2). And for stage 1, the duty will be 100%. For example, once V_{in} is measured as 18V, for stage 2 with V_{top} = 14.4V, we can easily set the PWM duty from the Eq. 11 of Appendix – I and Eq. 12 of Appendix – II.
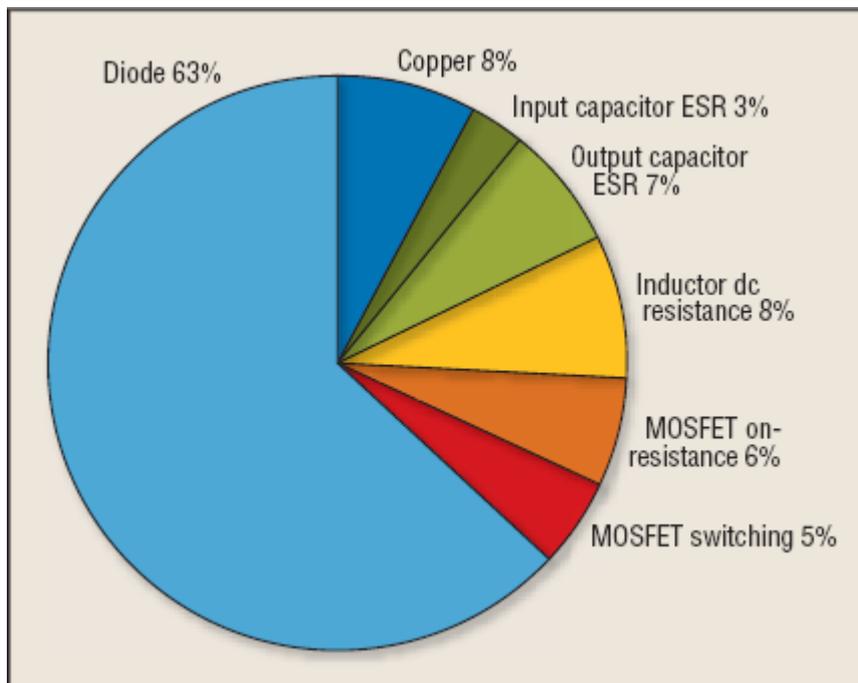

Fig. 3 Power loss caused by different elements of the device and the freewheeling diode.[4]

4. Conclusion

The goal of this design is to develop a lead acid battery charger, which is intelligent, automatic, takes care of battery health by constantly monitoring battery condition and compensate according to that. Though we have calculated most of the necessary data based on our requirement, however we can simply follow the design at [4] and use the values, as V_{out}=2V, which is nothing but a function of duty-cycle multiplied by V_{inMax}=24V as the worst case. It will work till it meets the input voltage and current ratings. Thus for our case, just using Eq 1, 2 and 11 is enough to get the perfect output voltage at specific stage with perfect environment condition. However, the calculation here (Appendix – II) can be used as an example and can help us to understand on designing the same charger for more current rating or larger battery banks.

The device proposed here is a modified version of [4] with feedback for self-control capability. The p-MOSFET and the freewheeling diode have been replaced by two n-MOSFETs as n-MOSFETs are low cost than p-MOSFETs. Also replacing the diode with a MOSFET increases efficiency [4] and Fig. 3 (which is Fig. 6 in [4]) tells us that diode causes a lot of power loss where MOSFET is relatively low-loss due to its low drain-to-source resistance. The study said a synchronous rectifier with MOSFET gives 85% efficiency.[4] Also the proposed design involves smaller number of low cost easily available components like the μC ATMega8, which very successfully replaces comparatively expensive and less available PWM driver. Choosing these commonly available components reduces the hassle of locally manufacturing the battery chargers for the 3rd world developing countries like Bangladesh. This charger can be used with Solar Chargers, car battery charging, backup power solutions like IPS/UPS, etc.

As the proposed device uses micro-controller, it is easy for the developers and manufacturers to program it for fulfilling exact need. Also it is easy to scale it up for larger current by just changing the inductor, capacitor and some minor code changes. For very large amount of current, parallel-connected MOSFETs can be used. Also as it is μC based, using RS232 or USB for communication between PCs is be possible. This will give us the flexibility of entering calibration data or programmability like setting mode/threshold current, etc by the manufacturer as after sales services. Also this can be menu driven for the same device in case of a

standalone charger. Further, more intelligence may be implemented based on battery chemistry, which is beyond this document.

5. Appendix – I

This part will cover all the necessary equations we need to develop a specific hardware design. The following equations have been used from [4].

$$L = (V_{inMax} - V_{out}) \times \frac{V_{out}}{V_{inMax}} \times \frac{1}{f_{sw}} \times \frac{1}{LIR \times I_{outMax}}$$;(Eq. 3); LIR = Inductor Current Ratio, 30% of I_{out}.[4]

Inductor's peak operating current:; $I_{PEAK} = I_{out} + \frac{\Delta I_{INDUCTOR}}{2}$ (Eq. 4)

Where, $\Delta I_{INDUCTOR} = LIR \times I_{outMax}$; (Eq. 5)

Output-voltage overshoot: $\Delta V = 100mV$;

For us, C_O is C2 in Fig. 2 Thus, Eq. 3 from [4] gives: $C2 = C_O = \frac{L(I_{PEAK})^2}{(\Delta V + Vout)^2 - (Vout)^2}$; (Eq. 6)

Output ripple due to the capacitance alone is: $V_{outCap} = \frac{1}{2C_O} \times \frac{V_{inMax} - V_{out}}{L} \times \left(\frac{V_{out}}{V_{inMax}} \times \frac{1}{f_{sw}} \right)$; (Eq. 7)

ESR of the output capacitor C2 (i.e. C_O) is:

$$V_{outESR} = I_{L_{ripple}} \times ESR_{C_O} = \Delta I_{INDUCTOR} \times ESR_{C_O}$$; (Eq. 8)

Total output-voltage ripple is:

$$V_{out_{ripple}} = (V_{outCap})^2 + \Delta I_{INDUCTOR} \times ESR_{C_O}$$; (Eq. 9)

Output ripple current is: $I_{C2_{ripple}} = I_{outMax} \frac{\sqrt{V_{out}(V_{in} - V_{out})}}{V_{in}}$; (Eq. 10)

Ref [8] gives us the equation for output voltage is: $V_{out} = kV_{in}$; (Eq 11) ; Where k is the duty cycle of the PWM.

6. Appendix – II

This part will give some specific values for a particular hardware design. As stated earlier, for ease of calculation and simplicity, we have used 12V 7Ah battery at 25^0C of temperature and the following:

V_{in} = 18VDC

V_{outMax} = V_{in} (100% duty cycle at V_{in})

The output voltage is our V_{top} or V_{float}. Thus for V_{top} = 14.4V, solving Eq 11 gives:

Duty-cycle, k=14.4/18=0.8=80% ; (Eq. 12)

Also for V_{float} = 13.4V, k=13.4/18=0.75=75% ; (Eq. 13)

Max output current = 7A

f_{sw} = 300kHz

From Eq. 3, L = 9.46uH = 10uH

From Eq. 4, I_{peak} = 8.05A. Thus for safety, we are choosing 10A as inductor saturation-current.

From Eq. 6, C2 = 250uF to 134uF. Thus we are choosing 470uF with keeping some tolerance for us.

Ref [4] says the input capacitor C1 = 10uF to 22uF per A, thus for us, we are choosing 47uF 50V capacitor for 3.49A of ripple current we got from Eq. 10.

Also we have selected power n-MOSFET like IRFZ44N or IRF540N, which is available in the market. The μC is commonly available ATMega8.

For shunt, a 0.1ohm 5W ceramic type resistor has been used here for measuring current. Also for larger current, a Closed loop or Open Loop Hall Effect Current Sensor is better than shunt as shunt also involves a lot of power loss. Thus in that case, a minor hardware and firmware change may require. Selecting proper Hall Effect Current Sensor will help us to design a common control board for a specific battery bank like 12V or 24V etc.

7. References

[1] (2012) The Battery University website. [Online] Available: http://www.batteryuniversity.com

[2] Figure 4-4: Charge stages of a lead acid battery. [Online] Available: http://batteryuniversity.com/learn/article/charging_the_lead_acid_battery

[3] (2012) The Battery University website. [Online] Available: http://batteryuniversity.com/learn/article/charging_the_lead_acid_battery

[4] Donald Schelle and Jorge Castorena, "Buck converter demystified", published in Power Electronics Technology Magazine, June 2006. [Online]. Available: http://www.powerelectronics.com

[1] Battery Temperature Sensor product datasheet, Blue Sky Energy. [Online]. Available: www.blueskyenergyinc.com

[5] (2012) The Battery University website. [Online] Available: http://batteryuniversity.com/learn/article/discharge_methods

[6] File: Lead-acid voltage vs SOC.PNG [Online] Available: http://en.wikipedia.org/wiki/File:Lead-acid_voltage_vs_SOC.PNG

[7] Muhammad H. Rashid, "Power Electronics Circuits, Devices, and Applications – 3rd Edition" ISBN: 978-81-317-0246-8

[8] (2012) The Wikipedia Website [Online] Available: http://en.wikipedia.org/wiki/Shunt_%28electrical%29

[9] Enne, R. and Zimmermann, H. "An integrated low power buck converter with a comparator controlled low-side switch", published in 13th IEEE Symposium on Design and Diagnostics of Electronic Circuits and Systems, April 14–16, 2010. [Online]. Available: http://ieeexplore.ieee.org/xpl/login.jsp?tp=&arnumber=5491813&url=http%3A%2F%2Fieeexplore.ieee.org%2Fstamp%2Fstamp.jsp%3Ftp%3D%26arnumber%3D5491813